Available online at www.sciencedirect.com
ScienceDirect
Progress in Natural Science 19 (2009) 983–989
Progress in Natural Science
www.elsevier.com/locate/pnsc

An atomistic simulation of site preference and vibrational properties of UM_xAl_{12-x} (M = Fe, Co, Ni, Cr and Mn) and $UM_xAl_{12-x}H_x$

Huijun Tian [a,b], Ping Qian [a,*], Jiang Shen [a], Nanxian Chen [a,c]

[a] *Institute of Applied Physics, Beijing University of Science and Technology, Beijing 100083, China*
[b] *School of Physics, Beijing University of Chemical Technology, Beijing 100029, China*
[c] *Department of Physics, Tsinghua University, Beijing 100084, China*

Received 14 July 2008; received in revised form 6 November 2008; accepted 12 November 2008

Abstract

A series of lattice inversion pair potentials are used to evaluate the phase stability and site preference for uranium intermetallics UM_xAl_{12-x} (M = Fe, Co, Ni, Cr and Mn) and their related hydrides. Calculated results show that Fe, Co, Ni, Cr or Mn atoms preferentially substitute Al at the 8*f* site. Interstitial H atoms only occupy 2*b* interstitial sites in UM_xAl_{12-x}. Calculated lattice constants are found to agree with a report in the literature. Elastic constants and bulk modulus of UM_xAl_{12-x} and $UM_xAl_{12-x}H$ were also investigated. In particular, the phonon densities of states (DOS) of these actinide compounds were evaluated for the first time.

Keywords: Interatomic potentials; Site preference; Lattice vibration

1. Introduction

The discovery of heavy fermion-like behavior in the UCu_xAl_{12-x} system [1,2] has aroused interest in the properties of its derivatives. These alloys crystallize in a $ThMn_{12}$-type tetragonal (*I*4/*mmm* SG) structure with four different crystallographic positions: uranium atoms occupy the 2*a* positions whereas Cu and Al atoms are located in the 8*f*, 8*i* and 8*j* positions. Since 1990, interstitial atoms such as H, C and N have been introduced into $R(Fe,M)_{12}$ compounds by a gas-solid phase reaction [3,4] and this has resulted in a dramatic change in magnetic properties of 1:12 compounds. Many experimental and theoretical studies have been carried out on R–Fe–X interstitial compounds [5–8]. It has been found that the introduction of both H and N increases the saturation magnetization and the Curie temperature as well as that N changes the easy magnetization direction of the rare earth sublattice. As for $R(Fe,M)_{12}H_x$, the magnetic properties of $RFe_{11}TiH$, $RFe_{11.35}Nb_{0.65}H$, $RFe_{12-x}Mn_xH$ and $HoFe_{12-x}Ta_xH$ have been investigated [9–12]. Very few data have been reported about the effects of hydrogen insertion on the physical properties of actinide compounds. We have previously reported structural properties for a series of rare earth compounds such as $R(M,T)_{13}$, $R_2(M,T)_{27}$, $R_3(M,T)_{29}$ (R = rare earth metals; M = Fe, Co, Al, Mn; T = transition metals) [13–20]. We thus extend our study to ternary uranium-iron-aluminum compounds UM_xAl_{12-x} (M = Fe, Co, Ni, Cr and Mn) and their related hydrides. Lattice vibrations of these compounds were of particular interest. The purpose of this work was to investigate properties such as site preference, elastic constants and the Debye temperature of these actinide compounds.

2. Theoretical methodology

2.1. The lattice inversion method

Over the last 10 years computational techniques have been applied extensively to the investigation of properties

* Corresponding author. Tel./fax: +86 10 62322872.
E-mail address: qianping@sas.ustb.edu.cn (P. Qian).

1002-0071/$ - see front matter © 2009 National Natural Science Foundation of China and Chinese Academy of Sciences. Published by Elsevier Limited and Science in China Press. All rights reserved.
doi:10.1016/j.pnsc.2008.11.008

Table 1
Morse parameters of some lattice inversion pair potentials.

	R_0 (Å)	D_0 (eV)	γ
U–U	3.9415	0.6624	7.3445
Al–Al	3.0059	0.4232	8.9191
Fe–Fe	2.7361	0.7640	8.7529
Mn–Mn	2.7889	0.8318	8.5108
U–Al	3.4682	0.5915	8.8707
U–Fe	3.2024	0.8835	8.6841
U–Ni	3.3033	0.7185	7.9600
Al–Mn	2.8729	0.6127	8.4451
Al–Ni	2.7212	0.5859	9.1625

and behavior of different materials. One of these techniques is atomistic simulation. The key problem with this technique is the determination of interatomic potentials. In the mid 1990s Chen used the Möbius inversion theorem from number theory to obtain interatomic potentials [21,22]. Methods for obtaining these potentials have been reported in our previous work [13–20]. The potentials are inverted from the cohesive energy and can be fitted simply by the Morse function

$$\mathbf{\Phi}(\mathbf{x}) = \mathbf{D}_0(\boldsymbol{e}^{[-\gamma(x/\mathbf{R}_0-1)]} - 2\boldsymbol{e}^{[-(\gamma/2)(x/\mathbf{R}_0-1)]}) \quad (1)$$

where D_0, R_0, γ are potential parameters. For the reader's convenience, several important potential parameters are listed in Table 1.

2.2. The second derivative method

Three basic methods are available for calculating mechanical properties according to the Cerius2 procedure provided by Materials Simulation Incorporated: second derivative, constant stress minimization and constant strain minimization. All these techniques can be used to obtain the stiffness matrix as well as its inverse referred to as the compliance matrix. These two matrices are then used to derive other properties such as Young's modulus, the bulk modulus, and Poisson's ratio. In this work, we use the second derivative method to acquire mechanical properties of uranium intermetallics.

The second derivative method uses a single point energy calculation to obtain second derivatives of the lattice energy with respect to lattice parameters and atomic coordinates. The following energy expression is used

$$U = U_0 + \sum_i \frac{\partial U}{\partial \varepsilon_i}\varepsilon_i + \frac{1}{2}\sum_{ij}\frac{\partial U^2}{\partial \varepsilon_i \partial \varepsilon_j}\varepsilon_i\varepsilon_j \quad (2)$$

where U_0 is the equilibrium energy and ε is the strain.

When the structure is at the minimum energy (i.e., all first derivatives of the lattice energy are zero), the second derivative term can be used to calculate the C_{ij} components of the stiffness matrix:

$$C_{ij} = \frac{\partial U^2}{\partial \varepsilon_i \partial \varepsilon_j} \quad (3)$$

The stiffness matrix computed by this method is always symmetric and thus $C_{ij} = C_{ji}$. The compliance matrix, S, is calculated as the inverse of the stiffness matrix:

$$S = C^{-1} \quad (4)$$

The volume compressibility is calculated from the compliance matrix as follows:

$$\beta = S(1,1) + S(2,2) + S(3,3) + 2[S(3,1) + S(2,1) + S(3,2)] \quad (5)$$

and the bulk modulus is the inverse of this volume compressibility:

$$B = \frac{1}{\beta} \quad (6)$$

3. Calculated results

3.1. The site preference of UM_xAl_{12-x} and their related hydrides

For the calculation the structural stability of alloys is judged by the minimum energy. The virtual binary UAl_{12} structure can be considered an intrinsic structure of UM_xAl_{12-x} (M = Fe, Co, Ni, Cr and Mn) compounds even though the UAl_{12} cell is essentially metastable. The calculation unit of UM_xAl_{12-x} was a $3 \times 3 \times 3$ cell (702 atoms in total) and was expanded from a $ThMn_{12}$ unit cell. In this process, we substitute Fe for Al atoms at each binary UAl_{12} compound site with different concentrations. The energy minimization method is then applied to relax the ternary system under the interaction of potentials. The average energy of final structures may thus be investigated and compared. We used 30 samples for each case where equivalent sites were randomly occupied by M (M = Fe, Co, Ni, Cr and Mn) atoms. The relationship between the crystal cohesive energy and the stabilizing elements content is shown in Fig. 1. The error bars denote the range of the root mean square error. After comparing these results it is obvious that the various values of cohesive energy correlate to the amount of M atoms and the three different types of Al crystallographic sites. Within the composition range $x < 4$, M atoms randomly occupy the 8*i*, 8*j* and 8*f* sites. The figure clearly shows that within $x < 4$ the cohesive energy is lower when Mn, Fe, Co, Cr or Ni atoms are substituted for Al at the 8*f* site rather than at the 8*j* and 8*i* sites. Mn, Fe, Co, Cr or Ni should thus have a preference for the 8*f* site in the $ThMn_{12}$ structure for $x < 4$. Site preferences in UM_xAl_{12-x} compounds are similar to those in Al-based rare earth compounds [19,20]. Based on the above analysis for the composition range $x > 4$ the equivalent 8*f* sites are fully occupied by M = Mn, Fe, Co, Cr or Ni atoms while the remaining M atoms will occupy the 8*j* or 8*i* sites. Calculated results show that the cohesive energy of UM_xAl_{12-x} decreases more rapidly with Fe, Co, Cr or Ni occupation of 8*i* sites than it does with Fe, Co, Cr or Ni occu-

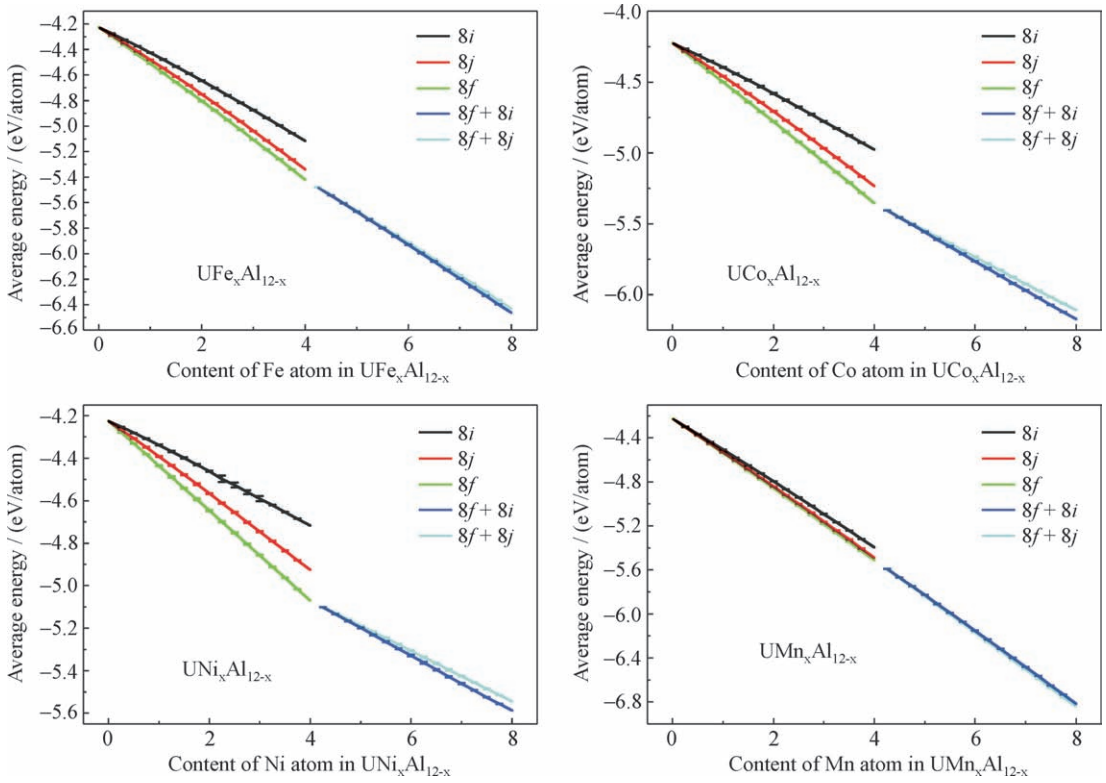

Fig. 1. Calculated cohesive energy variation with x when M atoms occupy different sites in UM_xAl_{12-x}.

pation of 8*j* sites. The Fe, Co, Cr or Ni atoms thus prefer 8*i* sites when $x > 4$ and when Mn atoms occupy 8*j* sites.

Calculated lattice constants of UM_xAl_{12-x} are listed in Table 2 together with experimental data from the literature [23]. Table 2 shows that our results agree with the experimental data. The calculated lattice constants are smaller than those of UAl_{12}. The largest deviation of a is 0.71% while that of c is 0.81%.

Fig. 2 shows that upon the introduction of interstitial H atoms the average energy decreases when H atoms occupy 2*b* sites and the addition of interstitial H atoms thus stabilizes $UM_xAl_{12-x}H$ structures. When H atoms occupy 4*c* sites the structure is unstable and the hydride does not retain its original structure. According to the calculations H atoms only occupy interstitial 2*b* sites in the $ThMn_{12}$-type structure. Fig. 2 shows that $UM_5Al_7H_x$ (M = Fe, Co, Cr and Mn) seems to possess a stronger ability to absorb hydrogen atoms. In Table 2 lattice constants of $UM_xAl_{12-x}H$ are shown and they all reproduce experimental data very well.

The stability of UM_xAl_{12-x} and their hydrides was investigated by a high temperature disturbance using molecular dynamics. We thus performed molecular dynamics simulations at constant pressure and temperature (*NPT*) with a $3 \times 3 \times 3$ periodic super-cell. For constant-*NPT* molecular dynamics the temperature and pressure were maintained constant using an extended system [24] with a thermostat and barostat relaxation time of 0.1 ps.

Table 2
Structural parameters a and c for UM_xAl_{12-x} and their related hydrides.

Compounds	a (Å)			c (Å)		
	Cal. (Å)	Exp. (Å)	Err. (%)	Cal. (Å)	Exp. (Å)	Err. (%)
UAl_{12}	9.2740			5.2790		
$UFe_{4.5}Al_{7.5}$	8.7450	8.7216	0.27	5.0692	5.0286	0.81
$UCr_{4.7}Al_{7.3}$	9.0468			5.2178		
$UFe_{4.7}Al_{7.3}$	8.7306	8.7141	0.19	5.0567	5.0274	0.58
$UFe_{4.85}Al_{7.15}$	8.7197	8.7061	0.16	5.0485	5.0245	0.48
UFe_5Al_7	8.6730	8.6976	0.28	5.0330	5.0224	0.21
UNi_5Al_7	8.7613			5.0080		
$UFe_{4.5}Al_{7.5}H$	8.7856	8.7233	0.71	5.0590	5.0287	0.60
$UMn_{4.5}Al_{7.5}H$	8.9404			5.085		
$UFe_{4.7}Al_{7.3}H$	8.7734	8.7168	0.65	5.0510	5.0285	0.45
$UFe_{4.85}Al_{7.15}H$	8.7645	8.7194	0.52	5.0410	5.0315	0.19
$UNi_{4.85}Al_{7.15}H$	8.8015			4.9900		
UFe_5Al_7H	8.7220	8.7021	0.23	5.0290	5.0243	0.09

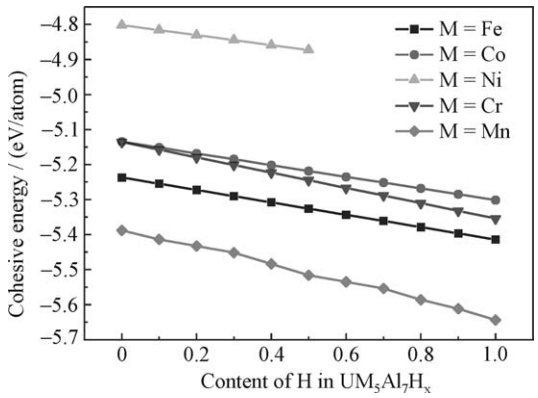

Fig. 2. Calculated cohesive energy of $UM_5Al_7H_x$ with H occupying the 2*b* site.

The simulation temperature range was 300–900 K with a step of 200 K. For each temperature and at 1 atm pressure calculations were performed for 30 000 steps with a time step of 2.0×10^{-15} s. After reaching equilibrium, the crystal symmetry retained the initial *I*4/*mmm* space group within a certain tolerance range at finite temperatures of 300–900 K. Lattice constants were found to change very little with respect to the temperature variation and the phase stability was thus verified.

3.2. Mechanical properties of UM_xAl_{12-x}

Difficulties in processing raw materials often make the experimental measurement of mechanical properties difficult and a very large computer capacity is required to calculate them by the *ab initio* method because of their complex structures. In this work we determined elastic constants and the bulk modulus of UM_xAl_{12-x} and their hydrides using the second derivative method based on the inverted pair potentials. Table 3 summarizes the calculated results. Table 3 shows that the calculated bulk moduli increase as Fe content increases for UFe_xAl_{12-x} and their hydrides. Bulk moduli of UM_xAl_{12-x} and elastic moduli of UFe_xAl_{12-x} have larger values than their hydrides, which demonstrate that the ternary elements M or interstitial H atoms play a role in determining the mechanical properties of these materials.

3.3. Vibrational properties of UM_xAl_{12-x}

Lattice dynamic properties of UM_xAl_{12-x} (M = Fe, Co, Ni, Cr and Mn) and their related hydrides were studied at an atomistic level using inverted interatomic potentials. Figs. 3 and 4 show computed results by considering the contribution to the DOS of the distinct atoms. From the partial DOS it may be inferred that the vibrational modes are mostly excited by Al atoms in the high frequency region. U and M largely contribute to modes with lower frequencies. U, however, only contributes to modes below 4.00 THz. The vibrational modes are almost excited by H atoms above 12.30 THz. In this work localized modes were analyzed qualitatively from interatomic potentials as shown in Fig. 4. For UCr_5Al_7 one Cr atom is present at the 8*i* site, eight Al atoms are at the 8*j* sites and four Cr atoms are at the 8*f* sites around U. Distances between U–Cr (8*i*), U–Cr (8*j*) and U–Cr (8*f*) are 3.19, 3.25 and 3.41 Å, respectively. Fig. 4 shows that U reacts strongly with Cr and Al at these distances. The mass of U is much larger than that of Al and is thus assumed motionless relative to the Al atom. Some Al atoms are restricted to the 'potential well' $\Phi_{U-Al}(r)$. This might be the reason for the appearance of Al-localized modes that correspond to the higher transected frequency. U atoms only contribute to lower frequency vibrations in the U–Al 'potential well' because of their large atomic mass. The interaction between U and Cr is, however, intense at their closest point (3.19 Å). Cr atoms cannot be excited by more modes with higher frequency compared to Al atoms because of the heavy mass of Cr. Furthermore, the nearest distance between Cr and Al is 2.62 Å and Cr thus reacts strongly with these Al atoms. This means that the Al atoms contribute to higher frequency modes because of the light Al. For $UCr_5Al_7H_{0.5}$ the optic modes are far separated from the acoustic modes and have very high frequencies which are due to the large mass difference in the atoms and the strong force constants between nearest neighbors Al or U and hydrogen atoms.

Table 3
Elastic constants and bulk moduli of UM_xAl_{12-x} and their related hydrides.

Compounds	Elastic constants C_{ij} (GPa)						Bulk modulus (GPa)
	C_{11}	C_{12}	C_{13}	C_{33}	C_{44}	C_{66}	
$UFe_{4.5}Al_{7.5}$	474	81	126	94	94	81	226
$UFe_{4.85}Al_{7.15}$	483	82	128	95	91	82	231
UFe_5Al_7	491	84	126	98	87	83	234
UCr_5Al_7	425	72	120	99	97	60	204
UCo_5Al_7	493	88	123	91	80	86	235
$UFe_{4.5}Al_{7.5}H$	470	75	113	78	78	63	221
$UFe_{4.85}Al_{7.15}H$	474	76	115	77	77	64	223
UFe_5Al_7H	487	81	110	78	72	63	228
UCr_5Al_7H	439	66	112	90	88	51	203
UCo_5Al_7H	501	84	114	76	69	73	232

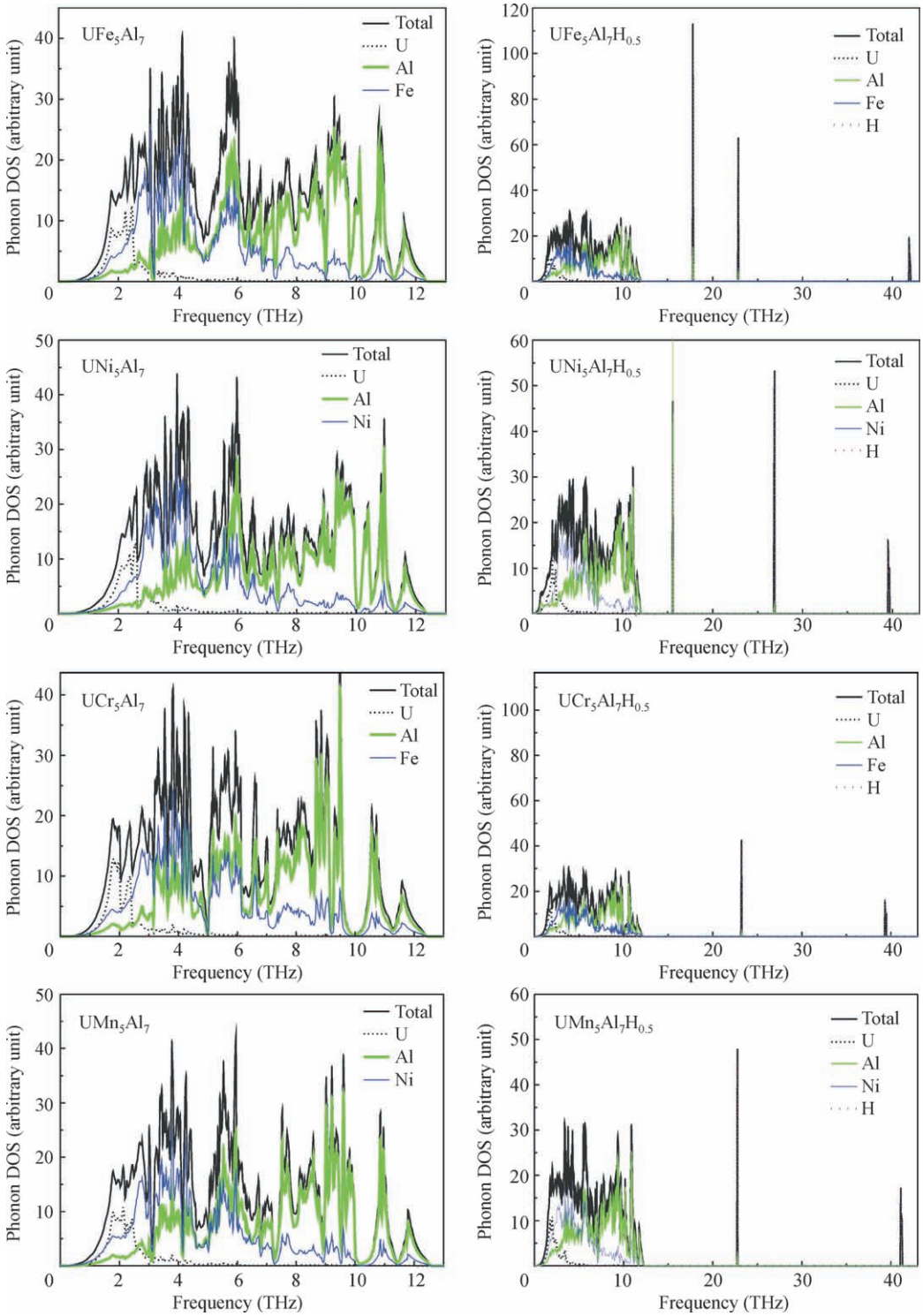

Fig. 3. Phonon densities of states of UM_5Al_7 (M = Fe, Ni, Cr and Mn) and their related hydrides.

The Debye temperature of a material is a suitable parameter to describe phenomena of solid-state physics that are associated with lattice vibrations. We used the expression:

$$C_v(T) = 3Nk_B \int_0^{\infty} \frac{(\hbar\omega/k_BT)^2 e^{\hbar\omega/k_BT}}{(e^{\hbar\omega/k_BT}-1)^2} g(\omega)d\omega$$

to calculate the lattice specific heat, $C_v(T)$, from our obtained lattice dynamic data as a function of temperature. In the conventional Debye model, the Debye temperature Θ_D can be defined as $\hbar\omega_m = k_B\Theta_D$. The specific heat is:

$$C_V = 3Nk_B(T/\Theta_D)^3 \int_0^{\Theta_D/T} \frac{x^4 e^x}{(e^x-1)^2} dx$$

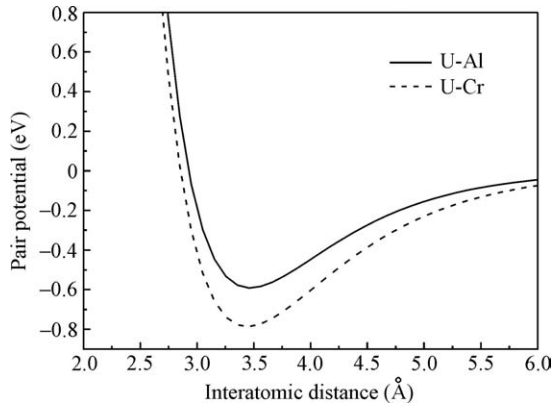

Fig. 4. Potential curves of $\Phi_{U-Al}(r)$ and $\Phi_{U-Cr}(r)$.

where $x = \hbar\omega_m/k_B\Theta_D$. Under $T \approx 0$ K, the Debye temperatures of UM_5Al_7 for M = Fe, Co, Ni, Cr and Mn are 457 K, 479 K, 481 K, 451 K and 486 K, respectively. The Debye temperatures of $UM_5Al_7H_{0.5}$ for M = Fe, Co, Ni, Cr are Mn are 434 K, 429 K, 449 K, 417 K and 430 K, respectively. Apparently, the Debye temperature decreases when interstitial H atoms are introduced into the UM_5Al_7 compound. H may, therefore, play an important role in lower temperature properties of these materials.

4. Conclusion

The structure, mechanical and thermodynamic properties of uranium intermetallics and their related hydrides are calculated using interatomic pair potentials obtained by the lattice inversion method. Calculated results demonstrate that M atoms preferentially occupy 8*f* sites. Interstitial H atoms only occupy 2*b* interstitial sites in UM_xAl_{12-x}. Calculated lattice parameters are similar to experimental values. The calculated results also suggest that this simple and promising method is useful for studying the properties of uranium intermetallics and their related hydrides.

The main advantage of this method is that these potentials are directly extracted from *ab initio* calculations without any experimental data and *a priori* potential function forms. The potential functions may thus be selected according to the shapes of inverted potential curves. This reduces some uncertainties in the derivation of pair potentials. However, due to a limit in the pair potentials form, we should point out that some properties that are dependent on many-body potentials may not be well described. Pair potentials did not yield satisfactory results for defects, vacancies and surfaces because structural local anisotropy deformation was not described correctly within the context of pair potentials. Consequently, three-body potential forms are to be introduced into future work.

Acknowledgements

This work was supported by the 973 Project in China (Grant No. 2006CB605101) and the Youthful Nature Science Foundation of Beijing University of Chemical Technology (Grant No. QN0618).

References

[1] Suski W, Wochowski K. Magnetic and electrical properties of the $UCu_{4-x}Mn_xAl_8$ alloys. J Alloys Comp 2001;317–318:395–7.
[2] Suski W, Czopnik A, Gofryk K, et al. $UCu_{4+x}Al_{8-x}$ and its derivatives. Solid State Sci 2005;7:784–90.
[3] Yang YC, Zhang XD, Ge SL, et al. Magnetic anisotropy and coercivity in RE–TM alloys. In: Proceedings of the sixth international symposium. Pittsburgh: Carnegie Mellon University; 1990. p. 190.
[4] Coey JMD, Sun H, Otani Y, et al. Gas-phase carbonation of R_2Fe_{17}; R = Y, Sm. J Magn Magn Mater 1991;98:76–8.
[5] Liao LX, Ryan DH, Altounian Z. Mossbauer determination of cobalt substitution in iron-based intermetallics. J Appl Phys 1991;70(10):6143–5.
[6] Zhang XD, Cheng BP, Yang YC. High coercivity in mechanically milled $ThMn_{12}$-type Nd–Fe–Mo nitrides. Appl Phys Lett 2000;77:4022–4.
[7] Yang JB, Mao WH, Yang YC, et al. Ab initio calculation of interstitial-atom effects in $YFe_{10}Mo_2X$ ($X = E$, H, B, C, N, O, F). Phys Rev B 1997;56:15647–53.
[8] Gaczynski P, Drulis H, Waerenborgh JC, et al. Mossbauer effect studies of RFe11Ti and RFe11TiH (R = Y, Gd, Er). J Magn Magn Mater 2006;302:503–10.
[9] Vert R, Fruchart D, Gignoux D, et al. On the new $RFe_{11.35}Nb_{0.65}$ (R = rare earth metals) alloys and their related hydrides and carbides. J Phys Condens Matter 1999;11(8,9):2051–7.
[10] Vert R, Bououdin M, Fruchart D, et al. Magnetisation and neutron diffraction studies of $HoFe_{12-x}Ta_xX_y$ ($0.5 \leqslant x \leqslant 0.7$, X = H, C). J Alloys Comp 1999;285(1–2):56–63.
[11] Shelyapina MG, Kasperovich VS, Baranov VS, et al. Characterisation by EPR analysis of the magnetic phase diagram of $RFe_{12-x}M_xX_y$ compounds (R = rare earth metal, M = transition metal, X = H, C). J Alloys Comp 2002;343(1–2):1–4.
[12] Piquer C, Grandjean F, Isnard O. An analysis of the hyperfine parameters of the RFe11Ti and RFe11TiH compounds, where R is a rare-earth element. J Phys Condens Matter 2006;18(1): 205–19.
[13] Chen NX, Shen J, Su XP. Theoretical study on the phase stability, site preference, and lattice parameters for $Gd(Fe,T)_{12}$. J Phys Condens Matter 2001;13:2727–36.
[14] Qian P, Chen NX, Shen J. Investigation of structural stability and site preference of $Dy(Fe,T)_{12}$ and $Dy(Fe,T)_{12}N_x$ (T = Ti, V, Cr, Nb, Mo). Intermetallics 2005;13:778–83.
[15] Qian P, Che NX, Shen J. Atomistic simulation for the phase stability, site preference and thermal expansion of $YFe_{12-x}T_x$ (T = Ti, V, Cr, Mn, Zr, Nb, Mo, W). Solid State Comm 2005;134:771–6.
[16] Chang H, Chen NX, Liang JK, et al. Theoretical study of phase forming of $NaZn_{13}$-type rare-earth intermetallics. J Phys Condens Matter 2003;15:109–20.
[17] Qian P, Chen NX, Shen J. Structural imitation and lattice vibration of $R_2Co_{17-x}Mn_x$ (R = Dy, Ho). Phys Lett A 2005;335:464–70.
[18] Li WX, Cao LZ, Shen J, et al. Effect of Mo content on the structure stability of $R_3(Fe,Co,Mo)_{29}$. J Appl Phys 2003;93:6921–3.
[19] Kang YM, Chen NX, Shen J. Lattice vibration of $Ce_{1-x}Sc_xFe_4Al_8$. J Phys Chem Sol 2003;64:433–41.
[20] Kang YM, Chen NX, Shen J. Atomistic simulation of the lattice constants and lattice vibrations in RT_4Al_8 (R = Nd, Sm; T = Cr, Mn, Cu, Fe). J Alloys Comp 2003;352:26–33.

[21] Chen NX, Ren GB. Carlsson–Gelatt–Ehrenreich technique and the Möbius inversion theorem. Phys Rev B 1992;45:8177–80.
[22] Chen NX, Chen ZD, Wei YC. Multidimensional inverse lattice problem and uniformly sampled arithmetic Fourier transform. Phys Rev E 1997;55:R5–8.
[23] Sério S, Waerenborgh JC, Goncalves AP, et al. Effect of interstitial hydrogen on UFe_xAl_{12-x}. J Alloys Comp 2001;317–318:88–91.
[24] Melchionna S, Ciccotti G, Holian BL. Hoover NPT dynamics for systems varying in shape and size. Mol Phys 1993;78:533–44.